

two distinct parts, firstly: ignition process, and secondly dimming operation. In the ignition process, the lamp is considered as an open circuit. Thus, during this operational stage, the series-resonant current through the ignition capacitor heats the two filaments and the voltage across the ignition capacitor ignites the lamp. On the other hand, during the dimming operation, the lamp is admitted as a variable resistance. In literature, several different models have been proposed to describe the behaviour of this equivalent resistance [9]. The calculated and measured lamp resistance versus lamp power is shown in Fig.2. Practical measurements were obtained from a simple 20 W fluorescent lamp. The calculated lamp resistance, obtained from [9]. Measured lamp resistance and the calculated lamp resistance agree well with each other when the lamp power is more than half of the full power. However, when the lamp power is low, there is a discrepancy between these two sets of figures.

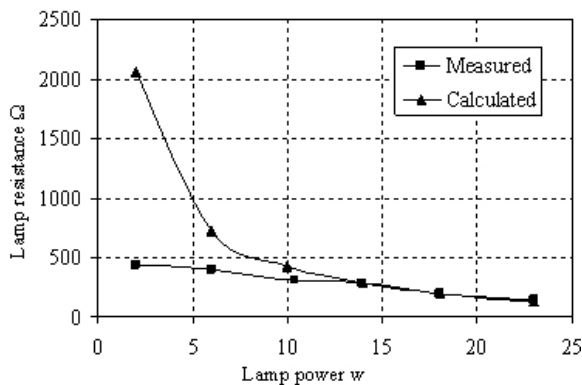


Fig. 2 Lamp equivalent resistance during dimming operation, at 24° C.

IV. SWITCHING OPERATION MODE

The step by step equivalent circuits of each mode are depicted in Fig. 3. Switches and diodes on-off states constitute each operation mode. Each operation mode is explained according to their circuit operation modes which are shown in Fig. 3. The value of circuit parameters and signal used for the simulation analysis are shown in table 1.

Mode 1 [t_0-t_1] ($S1$ is ON): $S1$ is in the on state. In this mode the DC-LINK voltage of V_{dc} lets the resonant circuit to accumulate energy by supplying power through $S1$ so resonant current through the lamp increases gradually. The inverter out-put power is controlled by the duration of this mode.

Mode 2 [t_1-t_2] (C_s is discharged): When $S1$ is turned off at $t = t_1$, the resonant current flowing through $S1$ begins flowing for a short period through the snubber capacitor C_s .

TABLE 1
CIRCUIT PARAMETERS OF THE PROPOSED $LCR C_{DC}$ PWM SOFT SWITCHING HALF BRIDGE INVERTER

Term	Symbol	Value
AC power supply	V_m	110 V, 50 Hz
Input filter inductor	$L_{f1} \& L_{f2}$	2mH
Input filter capacitor	$C_{f1} \& C_{f2}$	100 nf
DC-LINK capacitor	C	22 μ f
Switching frequency	f_s	20kHz
Lossless snubber capacitor	C_s	12nf
Resonant capacitor	C_r	22nf
DC blocking capacitor	C_{dc}	1 μ f
Resonant inductor	L_r	2.2mH

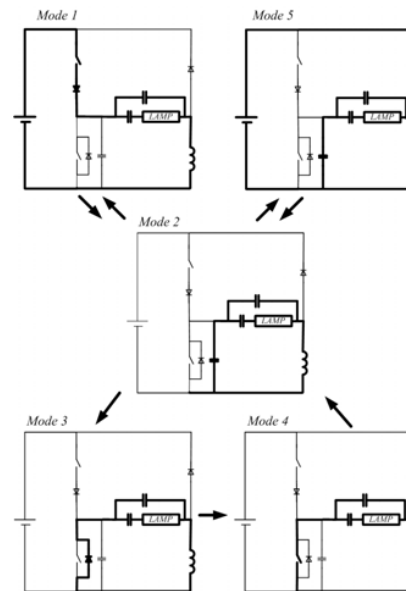


Fig. 3 Equivalent circuits in each switching operation mode.

In this process, a small amount of switching turn-off loss occurs when $S1$ is turned off while retaining some values in voltage and current. As $S1$ is turned off, C_s starts to discharge, and V_{S2} decays from V_{dc} to zero gradually. At the same time, V_{S1} rises from zero to V_{dc} gradually. Eventually, the anti-parallel diode $D2$ becomes on-state when the charging of C_s is finished. By conducting $D2$ this mode convert into mode 3.

Mode 3 [t_2-t_3] ($D2$ is ON): As the anti-parallel diode $D2$ starts to conduct, the voltage of $S2$ will reach zero. In this mode, the gate pulse voltage is applied to $S2$. While current of diode $D2$ reaches zero the switch $S2$ is turned on under ZVZCS conditions.

Mode 4 [t_3-t_4] ($S2$ is ON): Due to load resonance, the current freely resonates and flows in an inverse direction

through $S2$ which is already turned on. Here, the resonant capacitor, C_r , serves as a voltage source. The lamp current flows in the loop of $S2$, C_{dc} , R_{lamp} and L_r .

Mode 2 [t_4 - t_5] (C_s is charged): When $S2$ is turned off at $t = t_4$, the resonant current flowing through $S2$ starts to divert through the snubber capacitance C_s . In this process, a few amount of switching losses occurs at the turn-off transition. The resonant mode will continue until the voltage of inductor reaches to the DC-LINK voltage V_{dc} . From this time the auxiliary diode Da starts to conduct and this mode changes into mode 5.

Mode 5 [t_5 - t_6] (Da is ON): The auxiliary diode Da acts as a reverse recovery diode. In this mode, the stored energy of the resonant circuit is converted to DC-LINK voltage V_{dc} through diode Da . This diode does not have to be fast because it conducts inductive current. The turn-on and turn-off losses of diode Da are almost zero because the turn-on and turn-off transition occurs under zero voltage condition. Consequently, the auxiliary diode does not impose additional losses to the inverter. This mode is regarded as non resonance mode. The equivalent circuit of this mode is shown in Fig. 4. The diode current is approximated by linear waveform in order to simplify both the calculation and discussion. Therefore in calculation of power and energy recovery just the peak current of diode Da is considered. This peak value can be easily calculated from the initial current and voltage values of this mode. The voltage drop across Da during on state is negligible.

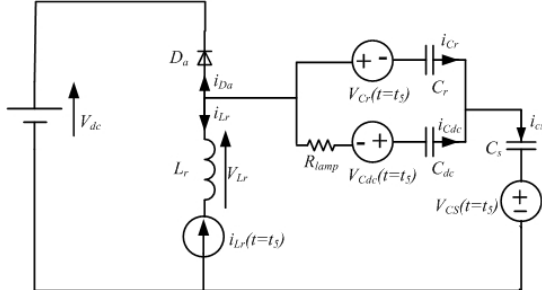


Fig. 4 Equivalent circuit of mode 5.

The initial diode current $i_{Da}(t = t_5)$ can be calculated as follows.

$$i_{Da}(t = t_5) = i_{Cs}(t = t_5) - i_{Lr}(t = t_5) \quad (1)$$

where $i_{Lr}(t = t_5)$ and $i_{Cs}(t = t_5)$ are the initial values of inductor (L_r) and capacitor (C_s) currents respectively. The value of $i_{Cs}(t = t_5)$ obtains from.

$$i_{Cs}(t = t_5) = i_{Cdc}(t = t_5) \frac{1}{(C_r / C_s) + 1} \quad (2)$$

Where $i_{Cdc}(t = t_5)$ is the initial value of capacitor (C_{dc}) current. The KVL in loop L_r , C_r and C_s , yields to

$$V_{Lr}(t = t_5) = V_{Cr}(t = t_5) + V_{Cs}(t = t_5) \quad (3)$$

Where $V_{Lr}(t = t_5) \approx V_{dc}$ and $V_{Cs}(t = t_5) = V_{dc}$ so the (3) yields to $V_{Cr}(t = t_5) \approx 0$ therefore initial capacitor C_{dc} current is obtain from

$$i_{Cdc}(t = t_5) = \frac{V_{Cdc}(t = t_5)}{R_{lamp}}$$

By defining the values of $i_{Lr}(t = t_5)$ and $i_{Cdc}(t = t_5)$ from pervious modes the value of $i_{Da}(t = t_5)$ can obtain from (1).

Equation (4) simplifies the calculation of the power that is sent from inductor to the DC-LINK voltage V_{dc} through diode Da .

$$P_r = \frac{1}{2} V_{dc} i_{Da}(t = t_5) f_s (t_6 - t_5) \quad (4)$$

Where P_r and f_r are the recovery power and switching frequency respectively. $(t_6 - t_5)$ is the duration of mode 5. Therefore, the reverse recovery energy, W_r , could approximately define as

$$W_r = \frac{1}{2} V_{dc} i_{Da}(t = t_5) (t_6 - t_5) \quad (5)$$

The average in-put power consumption is reduced by recovering this energy. As diode Da current falls to zero it goes to turn-off state and this mode convert into mode 2.

Mode 2: [t_6 - t_7] (C_s is discharged) In this mode C_s conducts to discharge the excessive energy and its voltage fell into the DC-LINK voltage V_{dc} . At t_7 , the switch $S1$ turns on and this mode returns to mode 1.

V. MEASURED SWITCHING OPERATION WAVEFORMS OF THE PROPOSED INVERTER

The observed waveforms of the switches, auxiliary diode Da , snubber capacitor C_s and the lamp at the duty cycle $D = 0.46$ are shown in Fig. 5. A 20W fluorescent lamp is used in laboratory prototype to measure these waveforms. It verifies the waveforms obtained by the simulations which will be show in Full Manuscript. Hence, the validated of the simulation becomes evident. In particular, switches $S1$ and $S2$ are found to turn-on under ZVS and ZCS operation.

Additionally, as can be seen from figures because of lossless snubber capacitor C_r , the switch, $S2$ is free from EMI but the switch, $S1$ has some oscillations. It should be noted that the diode peak current waveform is a little less than the one obtained from simulation. This is due to the assumption was made in the diode and resonant inductor that they are ideal. Moreover, unwanted oscillatory waveforms are observed in most of figures, which are not found in the simulation analysis. As can be seen in the Fig. 5(c), these phenomena occur at the turn-on times of the auxiliary diode. They probably come from the charges accumulated at the junctions of the diode, which may flow in an oscillatory way, owing to the capacitances of the diode and the stray inductances in the circuit etc. the oscillations at the instantaneous turn off and turn of the switches are inevitable, effected the current waveform of the snubber capacitor.

Additionally, as can be seen from figures because of lossless snubber capacitor C_r , the switch, $S2$ is free from EMI but the switch, $S1$ has some oscillations. It should be noted that the diode peak current waveform is a little less than the

one obtained from simulation. This is due to the assumption was made in the diode and resonant inductor that they are ideal. Moreover, unwanted oscillatory waveforms are observed in most of figures, which are not found in the simulation analysis. As can be seen in the Fig. 5(c), these phenomena occur at the turn-on times of the auxiliary diode. They probably come from the charges accumulated at the junctions of the diode, which may flow in an oscillatory way, owing to the capacitances of the diode and the stray inductances in the circuit etc. the oscillations at the instantaneous turn off and turn of the switches are inevitable, effected the current waveform of the snubber capacitor.

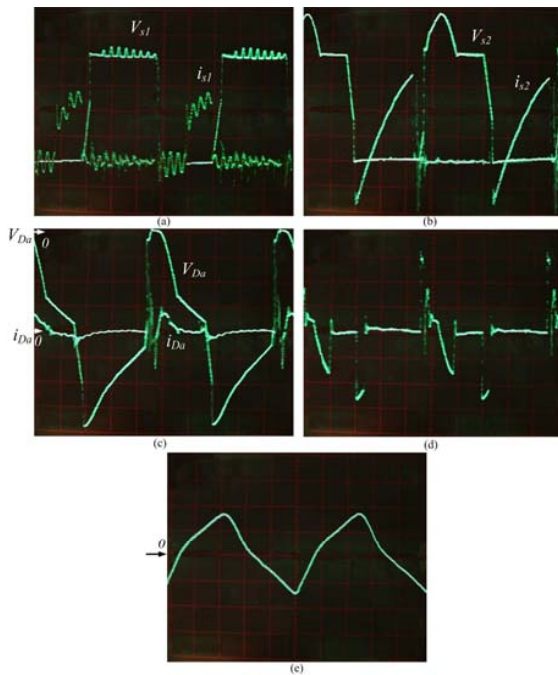


Fig. 5 Observed waveforms versus duty cycle. (a) Voltage and current of switch S1 (50 V/div, 0.2 A/div, 10 μ s/div). (b) Voltage and current of switch S2 (50 V/div, 0.2 A/div, 10 μ s/div). (c) Voltage and current of auxiliary diode (50 V/div, 0.1 A/div, 10 μ s/div). (d) Current of snubber capacitor (0.2 A/div, 10 μ s/div). (e) Lamp voltage (50 V/div, 10 μ s/div).

VI. ANALYSIS OF THE CONVERTER PERFORMANCE UNDER DIFFERENT LOAD CONDITION

In this section the converter behavior from output and input waveforms point of view is analyzed. In order to provide a good analysis, different fluorescent lamps with different length and wattage are used. A brief description of the lamps is depicted in the table 2. This description originates from experimental point of view.

TABLE II
LAMP PARAMETERS USED IN LABORATORY PROTOTYPE

fluorescent lamp	Lengh	Steady state resistance
40 W	1.2 m	352.60 Ω
20 W	0.5 m	148.0 Ω
15 W	0.35 m	82.750 Ω

VII. COMPARATIVE STUDY

Fig. 6 shows the DC to AC power conversion efficiency of the conventional and proposal

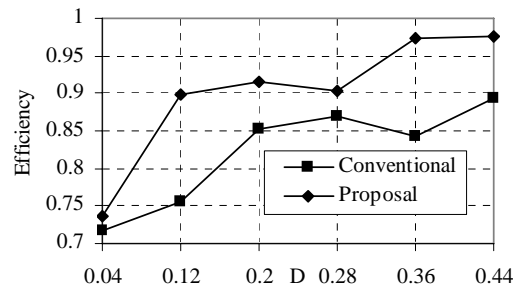


Fig. 6 DC-AC efficiency of conventional and proposal electronic ballasts against duty cycle D.

electronic ballast as a function of the duty cycle. These results are obtained from laboratory prototype which has got a 20 W lamp, mentioned in section 4, as its load. As can be seen, an extremely high efficiency of 99% is attained at $D = 0.36$ while the rated out-put is supplied. Also, a fairly high efficiency of about 90% is obtained at $D = 0.12$ when the minimum out-put power is feeding due to the soft switching of the switches. In addition, the soft-switching operation can be attained at a wide range of $0.1 < D < 0.44$.

VIII. CONCLUSION

In this paper a low switching losses LC_rC_{dc} series-parallel inverter using an auxiliary high frequency inverter has been presented. The inverter attains soft-switching operation and regulates its out-put power continuously over a wide range with the aid of a symmetrical PWM technique. Therefore, the electronic ballast provides high efficiency, low cost, small size and low energy consumption compared to the conventional electronic ballast. Examination of the experimental results confirm that wide dimming range and soft switching can be achieved over a wide duty cycle range in the proposed topology. The proposed converter offer great degree of flexibility in the variety load conditions which are provided with different lamp of wattage and resistance.

REFERENCES

- [1] Jesús Cardesín, José Marcos Alonso, Emilio López-Corominas, Antonio J. Calleja, Javier Ribas, Manuel Rico-Secades, and Jorge García, "Small-Signal Analysis of a Low-Cost Power Control for LCC Series-Parallel Inverters With Resonant Current Mode Control for HID Lamps," IEEE Trans. Power Electron., vol. 20, pp. 1205-1212, Sep. 2005.

- [2] [2] Sandra Johnson, and Regan Zane, "Custom Spectral Shaping for EMI Reduction in High-Frequency Inverters and Ballasts," IEEE Trans. Power Electron., vol. 20, pp. 1499-1505, Nov. 2005.
- [3] [3] J. Marcos Alonso, Antonio J. Calleja, Javier Ribas, Emilio López Corominas, and Manuel Rico-Secades, "Analysis and Design of a Novel Single-Stage High-Power-Factor Electronic Ballast Based on Integrated Buck Half-Bridge Resonant Inverter," IEEE Trans. Power Electron., vol. 19, no 2, pp.550-559, Mar. 2004.
- [4] B. Wang; X. Xiao," Application of multi-mode control strategy in the automotive HID headlight systems, " WCICA 2008 7th World Congress, June 2008, pp. 8064 - 8068
- [5] Z. Jian-dong, S. Zhi-yi; W. Zi-shang; W. Zhong-hua; "Research on integrated technology of intelligent control and electrical ballast for solar low pressure sodium lamp," IPEMC '09. IEEE 6th International May 2009, pp. 1259-1262
- [6] K. H. Liu and Y. L. Lin, "Current waveform distortion in power factor correction circuits employing discontinuous-mode boost converters," in Proc. IEEE PESC'89, 1989, pp. 825–829.
- [7] Stephen T. S. Lee, Henry Shu-Hung Chung, and S. Y. (Ron) Hui, "Use of Saturable Inductor to Improve the Dimming Characteristics of Frequency-Controlled Dimmable Electronic Ballasts," IEEE Trans. power electron., vol 19, pp. 1653-1660, Nov. 2004.
- [8] Manitoba HVDC Research Center, PSCAD/EMTDC: Electromagnetic transients program including dc systems, 1994.
- [9] F. T. Wakabayashi and C. A. Canesin, "A new model for tubular fluorescent lamps operated at high frequencies for dimmable applications," in Proc. IEEE ISIE'03, 2003.